XVIII. INTERACTION OF LASER RADIATION WITH PLASMAS AND NONADIABATIC MOTION OF PARTICLES IN MAGNETIC FIELDS[*]

Academic and Research Staff

Prof. D. J. Rose   Prof. L. M. Lidsky
Prof. T. H. Dupree   Prof. S. Yip

Graduate Students

J. D. Callen   D. E. Crane   R. W. Moir
H. Ching   M. D. Lubin   A. A. Offenberger

A. RADIATION-COOLED ARGON ION LASER

A discharge tube capable of containing high-current arcs has been developed. The device is especially well suited for use as an argon ion laser tube in the intermediate laser power range. The tube is entirely self-cooled by radiation. The capillary is constructed of dense high-grade alumina with excellent resistance to sputtering, high thermal conductivity, the ability to withstand high temperature, and high mechanical strength. This alumina is marketed under the trade name "Lucalox" by the General Electric Company. No vacuum-tight seals to the Lucalox are required. The current is supplied by thermionic emission from a hollow cathode. The anode was made identical to the cathode, to allow the possibility of running an AC discharge.

1. Design

The tube is shown in Fig. XVIII-1. The power dissipated in the capillary and in the electrodes is transferred entirely by radiation. An outer vacuum envelope of precision
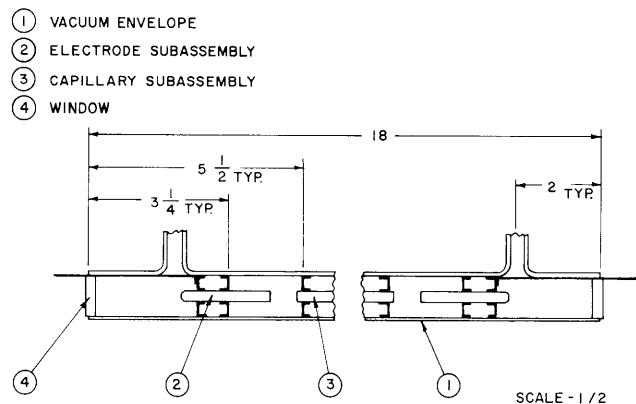

Fig. XVIII-1. Radiation-cooled laser.

bore quartz ① supports the electrode subassemblies ② and the capillary subassembly ③ by means of light press fits. The windows ④ are epoxied into the quartz envelope and are notched to allow passage of metal tape that forms the electrical leads to the electrodes. In Fig. XVIII-2 the capillary subassembly is shown inserted in the envelope.
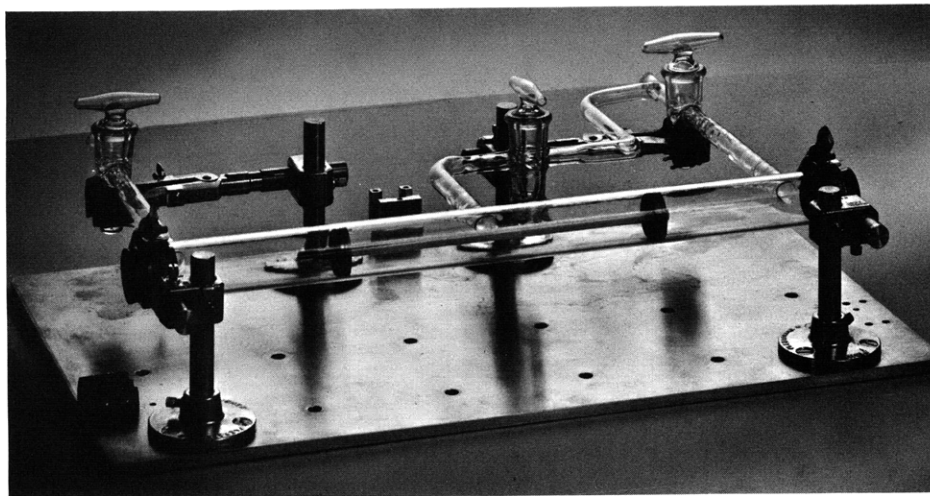

Fig. XVIII-2. Capillary subassembly.

The capillary subassembly consists of a $\frac{1}{4}$ inch O.D., $\frac{1}{8}$ inch I.D., $7\frac{3}{4}$ inches long, Lucalox tube, and the capillary supports, which were made of .010-inch niobium sheet. On one end the Lucalox was grooved and the support was rolled into the groove to provide a retainer. On the other end the Lucalox and support are fastened by means of a light press fit so that the Lucalox is free to expand and contract as the temperature changes. Niobium has a coefficient of thermal expansion that almost exactly matches that of Lucalox throughout the temperature range of interest.

The outer quartz envelope is precision bore with an I.D. of 1 inch and an O.D. of 1 3/16 inches. Quartz was used because of its large band for the transmission of electromagnetic radiation.

The electrodes were made of tantalum tubing, 2 1/2 inches long with an O.D. of 1/4 inch, and .010-inch wall thickness. The electrode supports were spun from .010-inch tantalum sheet to dimensions identical with the capillary supports, and were fastened to the electrodes by means of press fits. The electrical leads were made of .010-inch tantalum sheet cut into strips, 1/4 inch wide. Each lead was spot-welded to one of the electrode supports.

Means were provided to maintain the region between the capillary and the envelope at a pressure higher than that inside the capillary. This was done to insure that gas breakdown would occur only inside the capillary during start-up and operation.

2. Radiative Heat Transfer

The capillary and electrodes run at very high temperatures so that we need be concerned only with the emissive power of radiating bodies in which no radiation is returned. In this case the rate of heat transfer by radiation is given by the Stefan-Boltzmann law reduced by the total hemispherical emissivity ϵ, under the assumption that the monochromatic emissivity ϵ_λ is constant with wavelength. Then we have

$$\frac{q}{A} = \epsilon\sigma T^4,$$

where $\frac{q}{A}$ is the heat transfer rate per unit surface area, σ is the Stefan-Boltzmann constant, and T is the absolute temperature of the radiating body.

The inside wall of the capillary is limited to 1900°C, the stable temperature of Lucalox. Taking the temperature of the outer wall to be 2000°K, to allow for the possibility of local hot spots and for the temperature drop through the wall, the heat-transfer rate per unit length of capillary is found to be

$$\frac{q}{A} \approx 125 \text{ watts/cm.}$$

Approximately 25 per cent of this is absorbed in the vacuum envelope and then re-radiated, which results in a temperature of 625°C on the outside wall of the envelope.

3. Tube Characteristics

The tube was operated with an average fill pressure in the capillary of ~2.4 Torr argon. At this pressure the electric field in the arc is ~6 volts/cm for a tube of
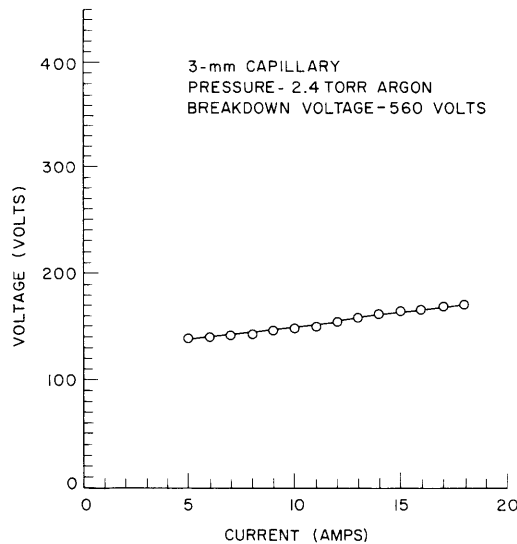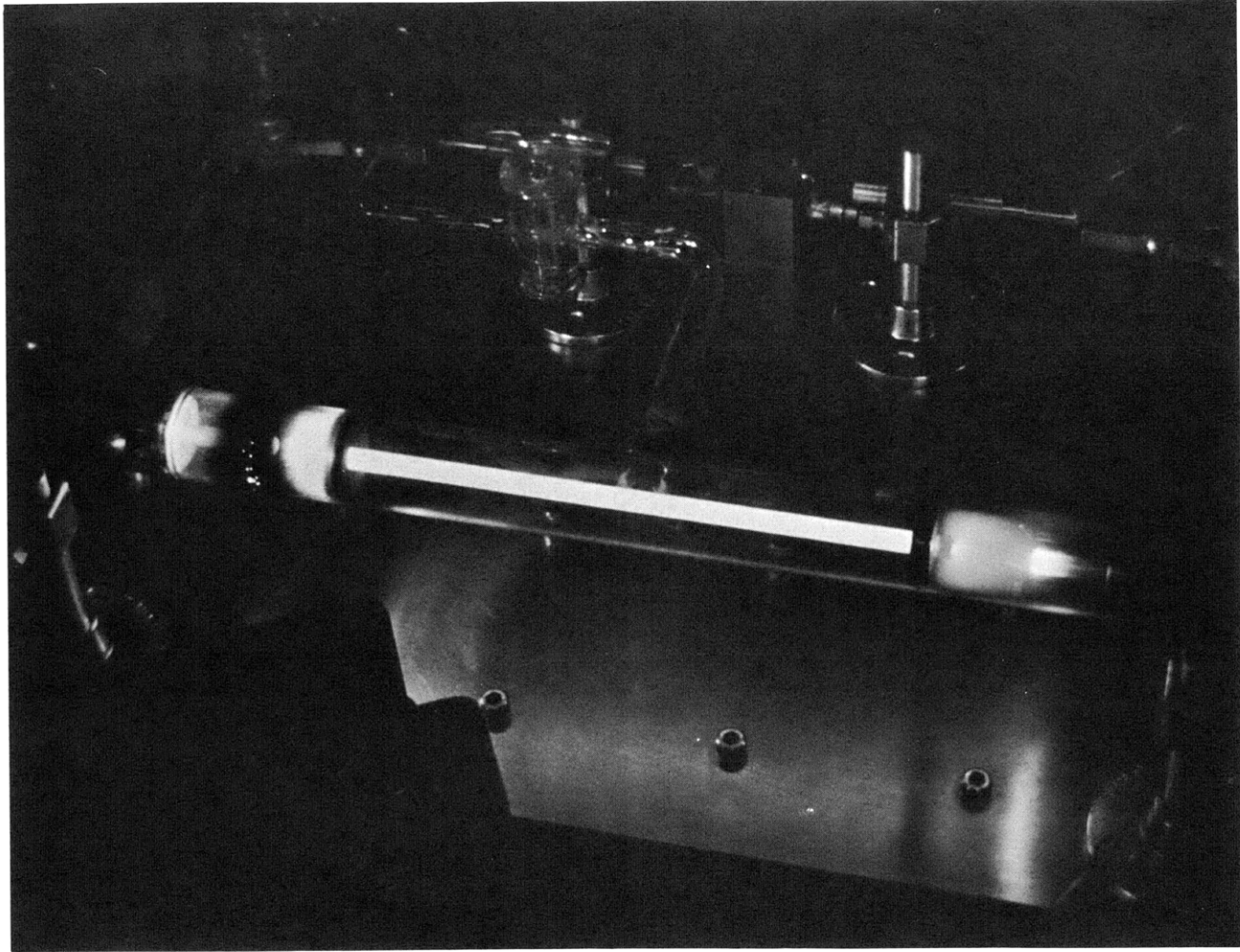

Fig. XVIII-3. Tube V-I characteristic.

Fig. XVIII-4.   Laser tube in operation.

3-mm diameter. Then the maximum safe operating current is predicted to be approximately 20 amps. The tube failed at a current of 18 amps, and melting of the capillary was observed near the anode; it is likely that the electric field was somewhat higher than 6 volts/cm.

The V-I characteristic of the tube is shown in Fig. XVIII-3 for an average fill pressure of 2.4 Torr argon. The slope is positive over the entire current range of the arc mode.

Figure XVIII-4 is a photograph of the tube in operation immediately preceding failure at 18 amps. At this point the total power dissipation in the tube was 3060 watts. The anode is on the left and the gas flow is from cathode to anode. The dark region at the cathode arises from sputtering from the cathode. Because of the sputtering, the transmission of radiation through the envelope was severely reduced, and high-speed fans were used to help cool the envelope at the cathode. Capillary temperature of a second tube (which failed from a trivial design fault) was 1525°C at 10 amps, which is consistent with our calculations and predictions for the device.

Optimum pressure for lasing in argon is ~0.3 Torr, for which the electric field in the arc is ~4 volts/cm for a 3-mm bore tube. Therefore, the tube should be capable of a discharge current of ~30 amps when operated as a laser.

The tube is well suited for many applications as an argon ion laser, since it is simple to construct and requires no water cooling. Refinements are also possible to make the device capable of handling much higher discharge currents, such as adding an axial magnetic field and attaching metal fins to the capillary to provide a larger surface area for radiation. Full details concerning the design and construction of the tube are available in D. E. Crane's thesis.[1]

<div align="right">D. E. Crane, D. J. Rose</div>

References

1. D. E. Crane, S.M. Thesis, Department of Nuclear Engineering, M.I.T., 1967.

B. RESONANT AND NONRESONANT DIFFUSION IN A HELICALLY PERTURBED MAGNETIC FIELD

During the last quarter, the diffusion measurements were extended to constant pitch helical perturbations that are applicable to nonadiabatic trapping experiments. A new kind of experiment was proposed for studying diffusion of electrons in either magnetic or electrostatic perturbation fields.

Diffusion of the electron's velocity was studied for the case in which a small transverse helical field is superimposed on the uniform field of a straight section of the torus. The field is specified by the uniform field B_o, the transverse field $B_\perp$, and the pitch of

the spatially rotating field P.

$$B_\perp = B_{\perp_0} \sin \frac{\pi z}{L} \tag{1}$$

$$P(z) = P_0. \tag{2}$$

Each time the electron moves around the torus it encounters the helical field, and $v_\perp$, its velocity transverse to B_0, changes.   This change can be computed by integrating the force equation along the trajectory.[1]

$$\Delta v_\perp = \int_0^L \omega(z) \cos \chi(z) \, dz \tag{3}$$

$$\omega_\perp(z) = \frac{q B_\perp(z)}{m},$$

where L is the length of the perturbation, and χ is the angle between the electron's posi-
tion and the direction of $B_\perp$. The spatial rate of change of χ is the difference between the
rate of change of the particle's angular position and the rate of change of the field direc-
tion.   The equation for χ, therefore, is

$$\frac{dx}{dz} = \frac{\omega}{v_z} - \frac{2\pi}{P} = \gamma. \tag{4}$$

Resonance occurs when $\gamma = 0$.   For small perturbations and the fields of Eqs. 1 and
2, Eq. 3 can be evaluated along the unperturbed orbit (that is, v_z = constant in Eq. 4).
Equation 3 then yields

$$\frac{\langle (\Delta v_\perp)^2 \rangle}{v_0^2} = Af(\gamma) \left(\frac{B_\perp}{B_0}\right)^2, \tag{5}$$

where

$$A = \left(\frac{\pi L}{r_0}\right)^2 ; \quad F(\gamma) = \frac{1 + \cos \gamma L}{\left[\pi^2 - (\gamma L)^2\right]^2} \tag{6}$$

$$r_0 \omega_0 = v_0$$

v_0 = electron speed.

The average sign < > is an average over the particle's phase at the entrance to the helical
perturbation. For $\Delta v_\perp$ independent of $v_\perp$, the number of transits is approximately N, with

$$N = \left\{ \frac{\dfrac{\left\langle (\Delta v_\perp)^2 \right\rangle}{v_o^2}}{\dfrac{v_{\perp 1 c}^2}{v_o^2}} \right\}^{-1}, \tag{7}$$

where $v_{\perp 1c}$ is the velocity at which the electrons are lost rapidly, because of the velocity-dependent nature of the drift compensation techniques employed.[1] When $\Delta v_\perp$ is dependent on $v_\perp$, an average over $v_\perp$ should be used in Eq. 7. If, instead of an average, we use the maximum value of $\Delta v_\perp$, then N in Eq. 7 is a lower limit.

The electrons are pulsed onto the magnetic axis of the torus and circulate around the torus until they diffuse to the walls.[1] The drifts are cancelled by means of an $\ell = 2$ helical coil on one U-bend, with a rotational transform of 100° and vertical fields adjusted to exactly compensate for the drift of a particle with $v_\perp = 0$.

The drift cancellation in the U-bends is velocity-dependent, and therefore a velocity space loss cone exists. We estimate for our case that $\dfrac{v_{\perp 1c}^2}{v_o^2} \approx 0.7$. When $\dfrac{v_\perp^2}{v_o^2} \approx 0.7$ the drifts in the U-bends are large, and the particles quickly intercept the charge collector.

We determine the number of transits by measuring the current collected in an annular charge collector as a function of time after the injection.

The electrons are injected with $v_\perp = 0$. This peaked distribution diffuses into a normal mode which then decays exponentially with a time constant equal to N. This time constant $N(B_\perp)$ is observed for a given perturbation field $B_\perp$, and represents scattering caused by nonadiabatic fields, gas scattering, and noncancellation of drifts. These scattering processes are independent of one another, and therefore the diffusion coefficients are additive, or equivalently the receprocal lifetimes are additive. The time constant $N(0)$ with $B_\perp = 0$ is observed. The time constant attributable to the perturbed field is N.

$$\frac{1}{N} = \frac{1}{N(B_\perp)} - \frac{1}{N(0)}. \tag{8}$$

Figure XVIII-5 shows the current from the charge collector as a function of time for different perturbation fields. The stronger field causes the particles to diffuse faster.

The case of a constant pitch perturbation (see Eqs. 1 and 2 with $P_o = 11.7$ cm) is shown in Figs. XVIII-6 and XVIII-7. From Fig. XVIII-6 we see that the behavior of N^{-1} is not square law (Eqs. 5 and 7) even for perturbation field $B_\perp/B_o$ less than 1 per cent. This is due to the fact that the unperturbed orbit does not represent the actual orbit

closely enough. The lifetime based upon unperturbed orbit calculations will be in error with strong perturbations; however, the error is always in a direction to give too small a lifetime, and hence will be useful as a lower bound.
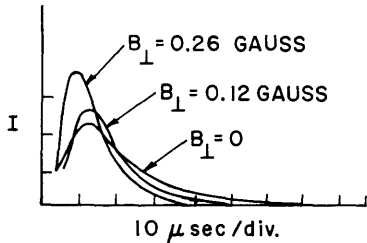

Fig. XVIII-5. Faraday collector current for several perturbation fields.

From Fig. XVIII-6 it is difficult to draw conclusions about the dependence of the diffusion coefficient on the perturbation field strength. In the case of a varying pitch helical perturbation, the dependence was verified to be $B_{\perp}^{3/2}$.[1] The strong field dependence for each value of B_z for the constant pitch helical field (Fig. XVIII-6) was $B_{\perp}$, with an exponent less than 3/2, which indicates a much stronger interaction.

Figure XVIII-7 shows the variation of the diffusion coefficient with B_z. When we increase the field B_z in Fig. XVIII-7, we decrease the pitch of the particle. At 70 Gauss the electrons with $v_{\perp} = 0$ are in resonance. At higher fields the electrons are never in resonance. As an electron diffuses, its velocity $v_{\perp}$ increases into $v_{\perp}$ space regions where the diffusion coefficient D_1, because of the helical field, is much reduced. But as $v_{\perp}$ increases, the diffusion coefficient D_2, attributable to the velocity dependence of the uncancelled U-bend drifts, increases. These two diffusion coefficients are shown in Fig. XVIII-8. D_1 is given by Eq. 5 and is proportional to $B_{\perp}^2$ when the lifetime is large (when $B_z > 80$ Gauss).

The diffusion coefficient (D_1+D_2) should be averaged over $v_{\perp}$ to predict the lifetime, namely

$$N = \frac{v_{\perp 1c}^2}{\frac{1}{v_{\perp 1c}} \int_0^{v_{\perp 1c}} \langle (\Delta v_{\perp})^2 \rangle \, dv_{\perp}}.$$

We expect the theory to be valid when N is large, say 100 or more. When D_1 is much larger than D_2 ($B_z < 80$ Gauss) the averaging becomes complicated. But when N, because of D_1, is larger than N(0) (N(0)≈100), the perturbation-induced diffusion is a small correction on the natural diffusion in the torus. In this case the experimental measurements are weighted by the ratio of D_1/D_2 (D_1/D_2 is rapidly varying), and thus the values are more indicative of diffusion at a single point in $v_{\perp}$ space. Therefore when B_z is above
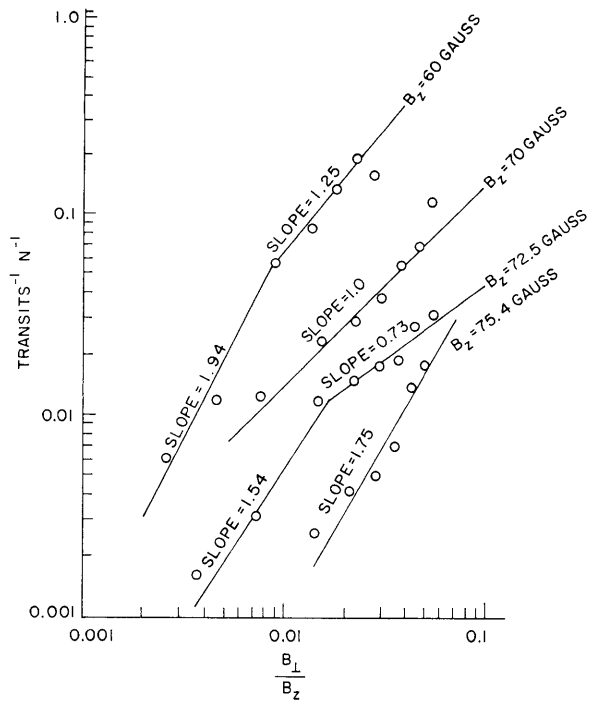
Fig. XVIII-6.
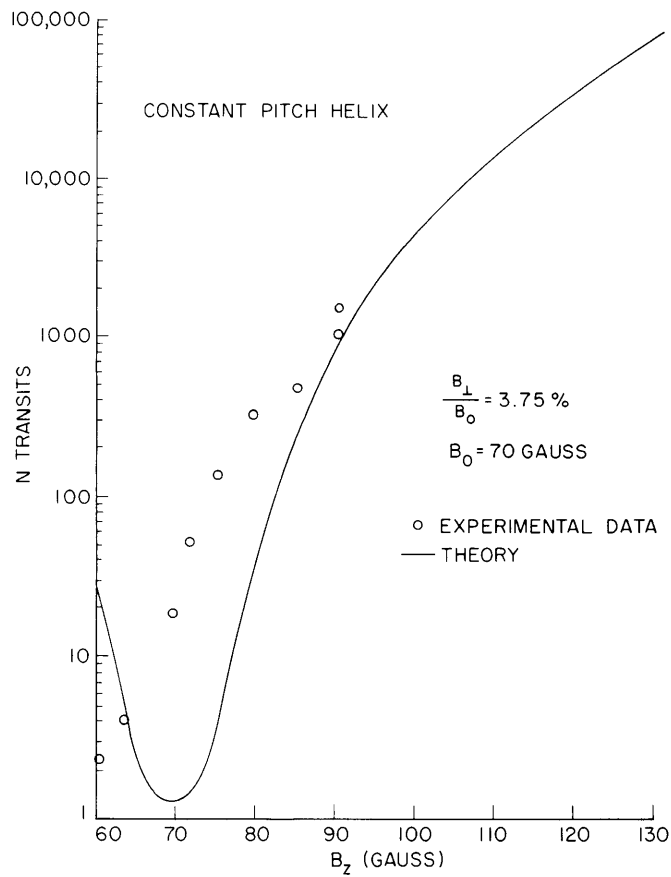
Diffusion coefficient vs helical field.
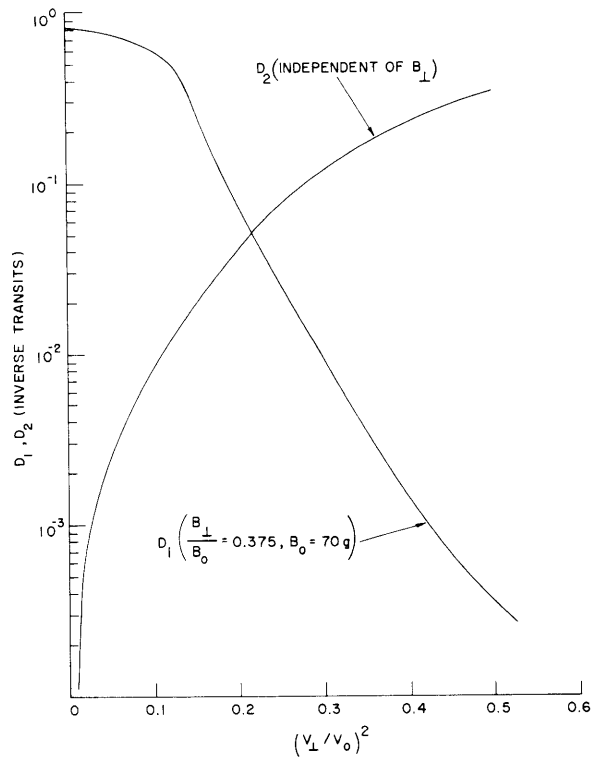
Fig. XVIII-7. Lifetime vs magnetic field strength.

Fig. XVIII-8.   Diffusion coefficients vs $v_\perp/v_o$.

~80 Gauss and N exceeds ~100, the theory and experimental data should agree. Figure XVIII-7 shows this agreement.

The diffusion coefficient (from Fig. XVIII-7) changes by a factor of 10^4 when the particle's pitch is decreased by a factor of 2, for example, by increasing B_z from 70 to 140 Gauss.   At 70 Gauss the experimental lifetime equals 18 transits; at 140 Gauss the theory curve, which is Eqs. 5 and 7 extrapolated, and the lifetime equals 18×10^4 transits.   This value of 18×10^4 transits is a lower bound, since the theory should be valid and the maximum value of the diffusion coefficient was used to obtain N.

As long as the behavior is diffusive in nature, we conclude that when the lifetime is long the unperturbed orbit solutions are valid, and $N \propto B_\perp^{-2}$, but when the lifetimes are short, the equations must be iterated a second time. Also, when the unperturbed orbit calculation is in error, it predicts too small a lifetime and hence gives conservative results.

1. Applications of Results to Nonadiabatic Molecular Ion Trapping with Breakup to Achieve Long-lived Atomic Ions

The diffusion coefficients were measured in a torus; however, they were characteristic of the perturbed field and not of the toroidal geometry.   Therefore

we can apply our results to the behavior of particles in a nonadiabatic magnetic-mirror trap.

We consider the problem of trapping a molecular ion beam in a magnetic-mirror device. We assume a perturbed field designed to increase the magnetic moment sufficiently on the first pass to trap the injected particles. As the molecular ions move back and forth through the perturbation from one mirror to the other, they diffuse in μ-space and are lost within a few tens of transits. A large fraction of the molecular ions will break up into atomic ions before the molecular ions are lost by nonadiabatic scattering if there is a strong breakup mechanism. One such mechanism is breakup on a 10^{12}/cc cold plasma produced by electron cyclotron heating.[2]

For purposes of illustration, we pick a system to analyze in which the experimental measurements can be scaled directly. As long as all dimensions are scaled linearly and the B field is scaled to give the same orbit sizes, our results from the experiment using electrons will be directly applicable to predictions of ion behavior. We consider a perturbation of the form of Eqs. 1 and 2 ($B_\perp$ = 375 Gauss, B_z = 10 kGauss, P_o = 35 cm, R = 5 = mirror ratio, 3 meters long). μ has been measured and found to be 0.23 after the first pass.

From previous experiments[3,4] we conservatively estimate the molecular ion lifetime to be 10 transits. Let the beam be 1 amp of 200 keV H_2^+. The density of H_2^+ is then given in terms of N, where N is the number of transits through the machine before being lost.

$$n = \frac{2\ell NI}{v_o \sqrt{1-\mu}\, q_o V}$$

I = 1 amp
N = 10
V = volume
n = 4.68×10^9/cc.

The lifetime of H_2^+, because of dissociation, is given by $\tau_{H_2^+}$, where

$$\tau_{H_2^+} = \frac{1}{n\sigma_{bi}v_{H_2^+}} = 15.4 \ \mu sec = 8.5 \ transits.$$

The lifetime is comparable to nonadiabatic scattering lifetime, and hence a large fraction (f) of the injected beam is dissociated into energetic ions. From our data and theory shown in Fig. XVIII-7, we see that the H^+ lifetime will be a factor 10,000 times longer than the H_2^+, 10^5 transits or 0.18 second. A more severe limit on the H^+ lifetime is charge exchange. If the neutral pressure can be maintained at 10^{-7} Torr, the charge exchange (σ_{ch} = 0.12 A^2) lifetime is 0.054 second. The charge exchange limited density is N_{H^+} = 7.7×10^{12}/cc. This density is high enough to warrant further study.

2. Proposed Wave-Particle Experiments

In order to measure the lifetime of very long-lived nonresonant particles, as well as short-lived resonant particles, we propose a new type of experiment for studying wave-particle interactions. This experiment consists of a long uniform magnetic field having electrostatic mirrors at both ends. A pulse of electrons is launched along the field lines and the mirrors are switched on when the electrons are between the mirrors. The electrostatic mirrors can be shaped so that adiabatic motion will occur. The only loss mechanism is gas scatter (there will be no ions and a very low density of electrons) which can be made very small at reasonably low pressures. A perturbed magnetic field (or electrostatic field) would be superimposed on the uniform field. The injected particles are peaked around their injected velocity and will diffuse in velocity space. After a time t, one mirror would be switched off and the electrons would be energy-analyzed. By this technique, one can measure the evolution of a distribution of particles in velocity space $f(v_{\parallel}, t)$. The diffusion coefficients can then be calculated from $f(v_{\parallel}, t)$.

The mirror fields must be charged to a potential exceeding the electron energy of 1500 volts, and the switching times must be much less than a transit time of 300 nsec. We have developed a pulse generator that will produce pulses of 1500 volts, with rise and fall times less than 20 nsec, which could be used in the proposed experiment.

The advantages of this system for studying wave-particle effects over previous systems is twofold. First, one obtains information about the whole distribution $f(v_{\parallel}, t)$, rather than just the distribution at the edge of the loss cone. Second, the particles will have a very long lifetime, thereby allowing very small perturbations to be studied (as in the case of nonresonant particles corresponding to dissociated H_2^+), as well as the strong perturbations.

R. W. Moir, L. M. Lidsky

References

1. R. W. Moir and L. M. Lidsky, "Electron Diffusion in the Helically Perturbed Magnetic Field of the M. I. T. Stellarator," Quarterly Progress Report No. 85. Research Laboratory of Electronics, M. I. T., April 15, 1965, pp. 225-229.

2. H. Lazar, D. Guest, and J. Dandle, ORNL-4080 (1967).

3. H. Dreicer, J. J. Karr, E. A. Knapp, J. A. Phillips, E. J. Stovall, Jr., and J. L. Tuck, Nucl. Fusion Suppl. Pt. 1, p. 299, 1962.

4. A. E. Robson, K. L. Aitken, D. A. Aldcroft, O. Lloyd and A. H. Morton, J. Nucl. Energy, Part C 9, 121 (1967).